Monofunctionalization and Dimerization of Nanoparticles Using Coordination Chemistry

Melissa R. Dewi,[†] Tina A. Gschneidtner,[‡] Sait Elmas,[†] Michael Ranford,[†] Kasper Moth-Poulsen,[*,‡] and Thomas Nann[*,†]

[†]ARC Centre of Excellence in Convergent Bio-Nano Science and Technology, Ian Wark Research Institute, University of South Australia, Mawson Lakes Boulevard, Adelaide, SA 5095, Australia and [‡]Department of Chemical and Biological Engineering, Chalmers University of Technology, Kemivägen 4, 41296 Gothenburg, Sweden

ABSTRACT This paper describes a strategy for controlled nanoparticle dimerization by using a solid support approach. Two types of nanoparticles have been linked by using a 5-([2,2′:6′,2″-terpyridine]-4′-yloxy)pentan-1-amine (terpy-amine) iron complex. The strategy includes two major steps: first, the monofunctionalization of individual nanoparticles with terpy-amine ligand molecules on a solid support, followed by release of monofunctionalized particles and subsequent dimerization. The versatility of the approach was demonstrated by dimerizing two different types of nanoparticles: spherical gold and cube-shaped iron oxide nanoparticles.

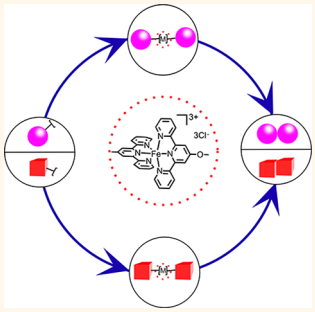

KEYWORDS: nanoparticles · colloids · nanostructures · dimerization · solid-state synthesis

Nanoparticles (NPs) are used for diverse applications ranging from magnetic resonance imaging (MRI),[1] drug delivery,[2] and bioimaging[3−5] over catalysis[6] to electronics[7] and sensing.[8] Most applications draw on their unique size- and shape-dependent chemical and physical properties. Endeavors to try and enhance the nanoparticles' properties have not ended at the level of individual particles—well-defined, self-assembled structures of different types of particles lead to new materials with enhanced properties. The most obvious way to create particles with new properties is probably by combining two different (or same) types of nanoparticles. The majority of research that has been undertaken in this area tries to combine two particles by exchanging (part of) their surface ligands and subsequent aggregation. Typical examples include Au−Au dimer nanoparticles,[9−11] Au−Cu_{2-x}Se heterodimers,[12] a PbS−Au nanoframe,[13] Cu−Fe_3O_4 heterodimers,[14] and Fe_3O_4−Ag heterodimers.[15] However, postsynthesis aggregation appears to be the main issue, which is difficult to control. Alternatively, dimers were synthesized *via* electrostatic interaction between two nanoparticles. Examples of dimers obtained by this approach are Ag−Pd, Au−Pd, Au−Au, and Au−Pd.[16] A third, very popular approach to synthesize heterodimer nanoparticles uses a seed-mediated method, where one type of NPs is grown onto the surface of another.[12−14] All of these methods have the benefit of resulting in a high yield of dimerization but are typically limited to certain types of nanoparticles and have little flexibility in the choice of materials. A recent review by Fernandez *et al.*[17] discusses the current state-of-the-art in the synthesis of nanoparticle dimers by self-assembly.

In order to combine two nanoparticles of choice (A and B of the same or of different materials), it is fundamentally important to have perfect control of the surface chemistry. The most straightforward strategy to achieve this is to first find a generic method to monofunctionalize nanoparticles (which means to functionalize them selectively on one face or side—not necessarily equip them with exactly one functional group) and then to dimerize exactly two particles. Recently, this area of research attracted much attention, especially the synthesis of so-called "Janus" particles by surface-enabled

* Address correspondence to kasper.moth-poulsen@chalmers.se, thomas.nann@unisa.edu.au.

Received for review October 13, 2014 and accepted December 10, 2014.

Published online December 10, 2014
10.1021/nn5058408

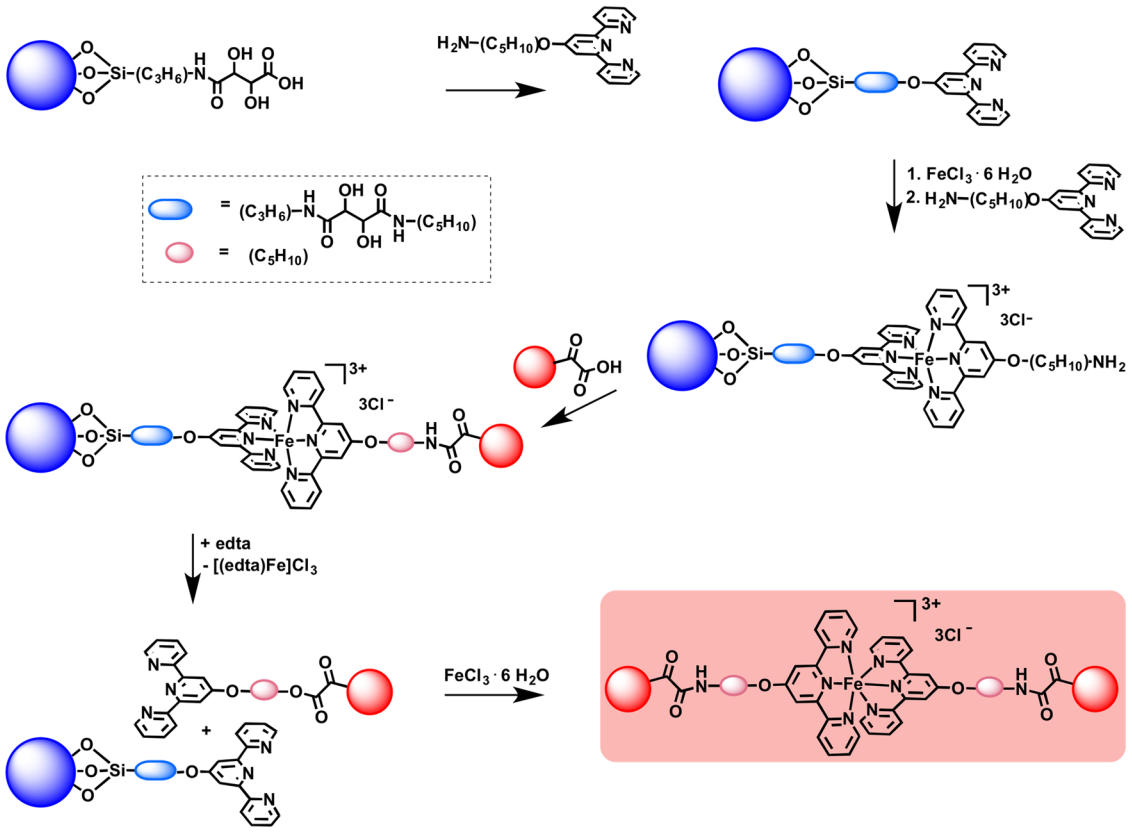

Scheme 1. Synthetic route for the synthesis of monofunctional NPs.

asymmetric functionalization.[18−24] Monofunctionalized nanoparticles are interesting for a range of applications including sensors[25] and single molecular electronics.[26] In this work, we have developed a method to monofunctionalize nanoparticles by using a solid support approach. The main difference in the work mentioned above is that we use a highly functional linker, which has the potential to perform the assembly/dimerization of nanoparticles reversibly. Furthermore, our approach is independent of the nanoparticles' surface chemistry and thus generally applicable. In a first step, we bound the nanoparticles onto larger SiO_2 particles. This was then followed by two steps of surface functionalization to passivate excess functional groups and cleave the particles from the solid support. The monofunctionalized NPs have been functionalized with amine-grafted terpyridine ligand molecules. To demonstrate the feasibility of our approach, we have successfully assembled our monofunctionalized Au and Fe_3O_4 nanoparticles into homodimers without any postsynthesis purification steps. Scheme 1 shows the step-by-step procedure to achieve monofunctionalized nanoparticles *via* our solid support approach.

RESULTS AND DISCUSSION

Uniform and well-defined Fe_3O_4 and Au nanoparticles have been synthesized following established protocols from the literature.[27−29] The nanoparticles were then assembled into dimers by using a sequential chemical functionalization of the nanoparticles and final complexation through 5-([2,2′:6′,2″-terpyridine]-4′-yloxy)pentan-1-amine (terpy-amine) chelating units. The reaction path depicted in Scheme 1 represents the synthetic route of this work.

In order to form dimers, the nanoparticles needed to be monofunctionalized. This aims to create just one active spot on the nanoparticles' surface to allow one-to-one conjugation *via* complexation linkage. To achieve this, functionalized nanoparticles have been bound to the surface of SiO_2 solid support particles by metal complexation. After subsequent decomplexation, we were able to obtain terpy-amine monofunctionalized nanoparticles (Scheme1).

The first step in monofunctionalizing nanoparticles involved the preparation of the silica solid support. Very rapidly, it became clear that commercial solid supports (*e.g.*, Merrifield-type resins) were not suitable for this work because these supports tend to "wrap" nanoparticles. Therefore, our system was built upon a more rigid silica nanoparticle platform. Terpy-amine ligands have been grafted onto carboxylated silica NPs by using the well-established 1-ethyl-3-(3-(dimethylamino)-propyl)carbodiimide/*N*-hydroxy succinimide (EDC/NHS) conjugation protocol (the detailed synthesis procedures of the silica solid support and FTIR spectra of

the intermediate stages can be found in the Supporting Information).[30] An excess of terpy-amine was used to ensure that all of the carboxylic acid groups of the solid support were converted. In the second step, $FeCl_3$ was complexed with the immobilized ligands, and subsequently, the anionic halides have been exchanged against non-immobilized terpy-amine ligands leading to a cationic octahedral iron bis-terpyridine complex, as depicted in Scheme 1. Then, carboxylate-functionalized NPs have been coupled to the free amine of the assembled linker using EDC/NHS as described above. Carboxy-functionalized Fe_3O_4[27] and Au[28] NPs have been prepared using methods that have already been published. The SiO_2 solid support particles turned from white to brown or pink-purplish in color when conjugated with Fe_3O_4 NPs and Au NPs, respectively. Transmission electron micrographs (TEM) of the resulting nanoparticles are shown in Figure 1.

Fourier transform infrared (FTIR) spectra of original Fe_3O_4 NPs, Au NPs, and SiO_2—Fe_3O_4 and SiO_2—Au nanostructures are shown in Figure 2. By comparing the FTIR peaks of the original Fe_3O_4, Au NPs, and their corresponding nanostructures, it is possible to investigate and determine whether or not the complexation has occurred.

Figure 2A depicts the spectra of oxalic acid capped Fe_3O_4 NPs prior to the conjugation process, which displays two prominent peaks at 1396 and 1610 cm^{-1}, which can be assigned to the O—H bend and C═O stretch vibrations, respectively. The peak at 3408 cm^{-1} can be assigned to the O—H stretch. Several new features appeared following the conjugation process, new peaks at 1099 cm^{-1} represent the SiO_2 solid support. Other peaks at 1559, 1653, 1701, and 3385 cm^{-1} can be assigned to the N—H bend (1°), C═O stretch, and N—H stretch of the amide bonds. The peak at 2983 cm^{-1} represents the C—H stretch of terpy-amine ligand molecules.

Similar new peaks are also found in SiO_2—Au nanoparticles, as can be seen from Figure 2B. A peak at 1095 cm^{-1} represents the SiO_2 solid support. Other peaks at 1567, 1644, 1704, and 3402 cm^{-1} can be assigned to the N—H bend (1°), C═O stretch, and N—H stretch of the amide bonds. The peaks at 2912 and 2989 cm^{-1} represent the C—H stretch of terpy-amine ligand molecules.

The resulting Fe_3O_4—SiO_2 and Au—SiO_2 nanostructures have been washed to remove unbound nanoparticles. In a final step, the monofunctionalized particles have been released from the solid support by using ethylenediaminetetraacetic acid (EDTA) to extract iron ions from the system's terpy-amine ligands. The cleaved SiO_2 solid support particles were then dissolved by adding 1 M NaOH.

The terpyridine-functionalized SiO_2 particles were poorly dispersible in common organic solvents and aqueous solutions. The best dispersibility was observed in dimethyl sulfoxide (DMSO). The nuclear magnetic resonance (NMR) spectroscopic investigation of the terpyridine silica particles in DMSO-d_6 revealed the successful immobilization of the terpyridine amine ligands onto the SiO_2 surface by amide coupling. Figure 3 shows the aromatic region of the stacked ^1H NMR signals of the unmodified and immobilized terpyridine amide ligand in DMSO-d_6. As depicted in the spectrum, the ^1H NMR signals of the aromatic protons became broadened due to the immobilization and loss of the symmetry. Where the singlet caused by both protons of the central pyridine ring at 7.9 ppm and the multiplets, between 8.50 and 8.70, remained

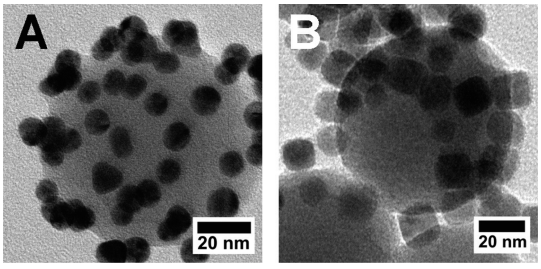

Figure 1. TEM micrographs of (A) SiO_2—Au nanoparticles and (B) SiO_2—Fe_3O_4 nanoparticles.

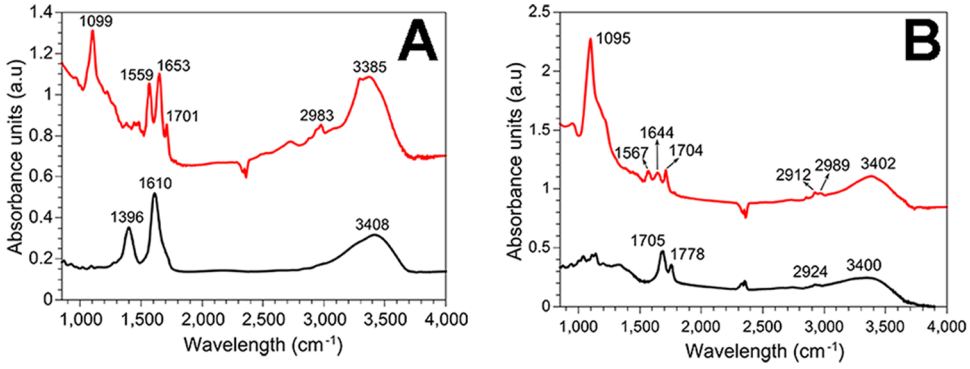

Figure 2. FTIR spectra of (A) Fe_3O_4 monomers functionalized by carboxyl (—COOH) groups from oxalic acid (black), whereas the red line represents the FTIR spectra of SiO_2—Fe_3O_4, and (B) Au monomers functionalized by carboxyl (—COOH) groups from 3-MPA (black), whereas the red line represents the FTIR spectra of SiO_2—Au.

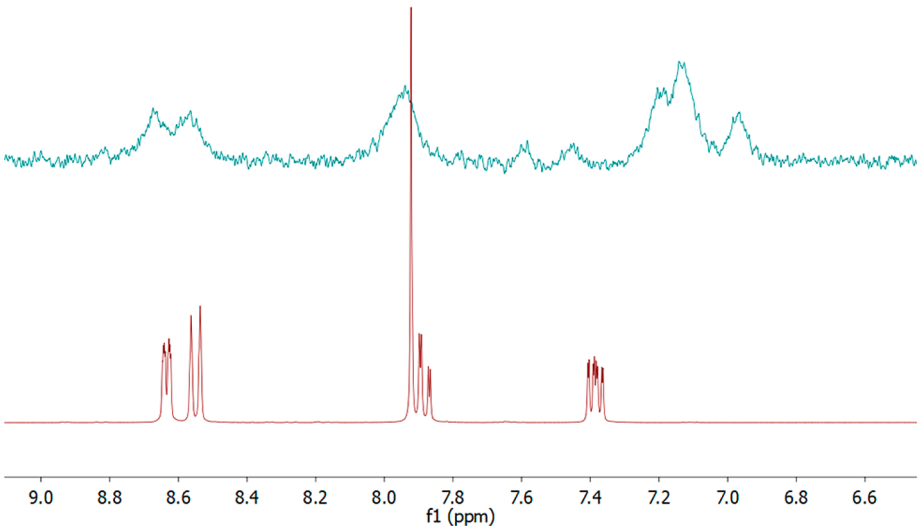

Figure 3. ^{1}H NMR spectrum (aromatic region) of the terpyridine amine as pure (red spectrum) and immobilized ligand (green spectrum) in DMSO-d_6.

unchanged after immobilization, the ^{1}H NMR multiplets at 7.85 and 7.38 showed high-field shifts from at least 7.40 ppm to less than 7.00 ppm, indicating a strong electron-pushing effect of the silica particles to the terpyridine units. Due to the poor dispersibility of the modified ligand, the aliphatic protons of the terpy-amine unit disappeared under the strongly broadened solvent peak of DMSO-d_6. Typically, the latter protons adjacent to the amide unit are expected to show the strongest impact after immobilization.

Figure 4 shows a TEM overview of Fe_3O_4 and Au nanoparticle dimers (dNPs). The TEM micrographs signify that Fe_3O_4 and Au dimer nanoparticles have been formed by terpy-amine–Fe complex linkages. The sizes of the dNPs fall within the optimum size range for diverse applications.[31] In addition, the TEM micrographs indicate that dNPs are well-dispersed in aqueous solution (in this case, water) since no larger aggregates were observed.

Figure 4E,F display high-resolution TEM (HR-TEM) micrographs of individual Fe_3O_4 and Au dimers. It can be clearly observed that the aforementioned metal complex has coupled the two individual nanoparticles, as the distance between the two nanoparticles was very small. In addition, the lattice fringes of Au dNPs and Fe_3O_4 dNPs can also be observed, and these are in good agreement with the expected metallic gold and magnetite iron oxide lattice spacings of 2.4 and 2.9 Å, respectively. The yield of the dimerization reaction was estimated by analysis of the TEM micrographs (results can be found in the Supporting Information section 8). For example, for the Au NPs, an overall percentage yield of approximately 50% was found. However, the formation of some trimers has also been detected. This might be a consequence of failing to achieve monofunctionalization (having more than one functional spot on the nanoparticles' surface). A 58% yield has been achieved in the case of Fe_3O_4 nanoparticle dimers. It was found that selective dimerization competes with random aggregation. To prevent this, dimerization had to be performed in dilute dispersion, which then limited overall yield of the reaction.

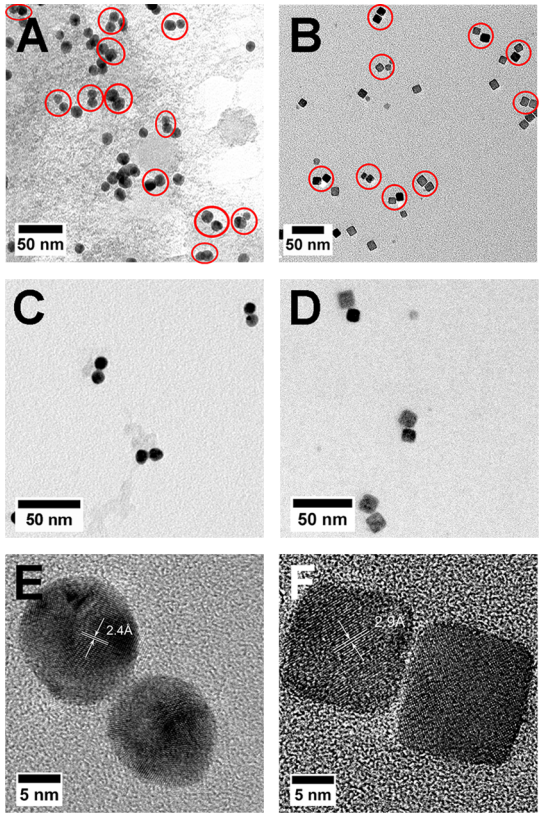

Figure 4. TEM micrographs of (A,C) Au and (B,D) Fe_3O_4 dimers. HR-TEM micrographs of Au dimers (E) and Fe_3O_4 dimers (F).

The absorption spectra of the Au–Au dimers have been measured to investigate the absorption band

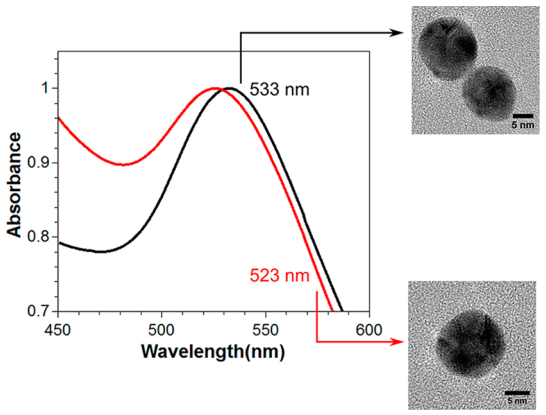

Figure 5. UV−vis absorption spectra of Au NPs (red graph) shows an absorption peak at 523 nm. This is a typical absorption peak of colloidal gold nanoparticles. The dimer formation results in a red shift of the original absorption peak toward the infrared range (533 nm, black graph). This suggests the increased size as two individual Au NPs have been joined together *via* terpy-amine−Fe complex linkages.

shift on dimerization (Figure 5). The absorption peak at 523 nm for Au NPs corresponds to the plasmon resonance of colloidal gold nanoparticles. For the dimers, the corresponding absorption peak has been shifted approximately 10 nm toward the infrared region, which indicates the increased size of the nanoparticles (formation of Au−Au dimers).

CONCLUSIONS

In conclusion, nanoparticle dimers of spherical gold (Au) and cube-shaped iron oxide (Fe_3O_4) particles have been formed by using 5-([2,2′:6′,2″-terpyridine]-4′-yloxy)pentan-1-amine/amine grafted terpyridine as ligand molecules to connect two monofunctionalized nanoparticles by metal complexation. The successful assembly of Au and Fe_3O_4 nanoparticle dimers demonstrated the versatility of the approach. We expect that this new bottom-up approach for the formation of homodimers will pave the way for future complex nanoarchitecture and new applications. Using a metal complex for coupling two nanoparticles could also allows for reversible dimerization by removing the central metal ion selectively in the future.

MATERIALS AND METHODS

Carboxylated silica (SiO_2) nanoparticle solid supports of approximately 50 nm diameter were synthesized by using the well-known Stöber method. Spherical gold nanoparticles have been synthesized by a seeded growth method followed by surface functionalization (please refer to the Supporting Information for details). Cube-shaped iron oxide nanoparticles (Fe_3O_4) have been synthesized by a thermal decomposition method, following the work which has been performed by Dewi *et al.*[27]

Step 1: Terpy-amine-functionalized silica nanoparticles have been prepared through carbodiimide (CDI) conjugation. A total of 10 mL of carboxy-functionalized SiNPs from the aforementioned synthesis were dried and redispersed in ∼8 mL of DMSO (44 mg/mL). To activate the surface functional COOH groups, 81 mg/mL of CDI in DMSO was added to the SiNP dispersion, and the mixture was vigorously stirred at 50 °C for 2 h. Carboxylate-activated SiNPs were then purified by centrifugation to remove excess conjugation agents with DMSO at 15 000 rpm for 15 min. Then, the nanoparticles were homogeneously dispersed in 8 mL of DMSO. Into this dispersion (8 mL of terpyamine-functionalized SiNPs) was added 19.50 mg of terpy-amine in 8 mL of DMSO (please refer to the Supporting Information section 7) and vigorously stirred at room temperature for 24 h under N_2 atmosphere. Terpy-amine-activated SiNPs were purified by centrifugation to remove unbound terpy-amine with DMSO at 15 000 rpm for 15 min and redispersed in 8 mL of water.

Step 2: To allow monofunctionalization and complexion of terpy-amine-functionalized SiNPs with unbound terpy-amine ligand molecules, it was necessary to introduce metal complexes ($FeCl_3 \cdot 6H_2O$) into the system to create such structures. Into the dispersion, was added 15.70 mg of $FeCl_3 \cdot 6H_2O$ in 8 mL of DMSO, and the mixture was vigorously stirred for ∼15 min at room temperature. The mixture was centrifuged at 15 000 rpm for 15 min and redispersed in 8 mL of DMSO. Furthermore, 19.50 mg of unbound terpy-amine in 8 mL of DMSO (please refer to the Supporting Information section 7) was added to the above complexed mixture and stirred for ∼15 min at room temperature. The mixture was centrifuged at 15 000 rpm for 15 min in 8 mL of water.

Step 3: As-synthesized NPs (Fe_3O_4 and Au) were surface-functionalized with oxalic acid ($C_2H_2O_4$) and 3-mercaptopropionic acid, 3-MPA ($HSCH_2CH_2CO_2H$), respectively, to feature carboxylate groups (−COOH), while SiNP solid support templates feature terpy-amine ligand molecules. In order to bind the NPs to the solid silica support, 100 μL of terpy-amine-functionalized SiNPs was mixed with 100 μL (50 mg/mL) of Au-MPA NPs, and the mixture was diluted by addition of 4.8 mL of water. Into the system was quickly added 0.3 mmol of NHS and EDC. The mixture was then reacted at room temperature for 3 h. After reaction, the resulting mixture was centrifuged at 15 000 rpm for 15 min and washed twice with water. An identical procedure was employed to Fe_3O_4 NPs. After purification, both SiO_2−Au and SiO_2−Fe_3O_4 nanostructures were redispersed in 1 mL of water.

Step 4: An aqueous solution (1 mL) of EDTA (0.213 mg/mL, ethylenediaminetriacetic acid) was added to the terpy-amine-functionalized SiNP solution. The mixture was stirred for ∼15 min at room temperature. To segregate the passivated Au and Fe_3O_4 NPs from the SiNP solid support templates, 2 mL of NaOH (1 M) was added into 1 mL of SiO_2−Au nanostructure solution. The resulting mixture was then sonicated at 50−60 Hz for about 30 min to dissolve the SiNPs. After sonication, the NP mixture was centrifuged at 15 000 rpm for 10 min and the supernatant was discarded. The resulting precipitate was then redispersed in 1 mL of water.

Dimerization. Into the mixture of 1 mL of monofunctionalized Au NPs was added 0.2 mg of $FeCl_3 \cdot 6H_2O$ in 1 mL of DMSO, and the mixture was stirred for ∼15 min at room temperature to allow adequate time for dimerization. The same approach was taken with Fe_3O_4 NPs: into 1 mL of monofunctionalized Fe_3O_4 NPs was added 0.2 mg of $FeCl_3 \cdot 6H_2O$ solution and stirred for ∼15 min at room temperature. After reaction, the mixture was then centrifuged at 15 000 rpm for 15 min, and the resulting precipitation was washed with water twice and finally redispersed in 2 mL of water for storage.

Conflict of Interest: The authors declare no competing financial interest.

Acknowledgment. This research was partly conducted and funded by the Australian Research Council Centre of Excellence in Convergent Bio-Nano Science and Technology (project number CE140100036). T.A.G. and K.M.-P. acknowledge support from Chalmers Materials area of advance as well as the European research council (ERC-StG 337221 SIMONE). M.R.D., S.E., M.R., and T.N. would like to acknowledge Dr. Amelia Liu

from Monash Centre for Electron Microscopy, Melbourne, Australia, for the useful help with TEM imaging. Part of this research was also supported by the Australian Microscopy and Microanalysis Research Facility (AMMRF). Another part of this work was performed at the South Australian node of the Australian National Fabrication Facility, a company established under the National Collaborative Research Infrastructure Strategy to provide nano and microfabrication facilities for Australia's researchers.

Supporting Information Available: Further details on the experimental methods, analytical data not shown in the main text, and calculations to obtain optimum reagent concentrations as discussed in the main article. This material is available free of charge *via* the Internet at http://pubs.acs.org.

REFERENCES AND NOTES

1. Sun, C.; Lee, J. S.; Zhang, M. Magnetic Nanoparticles in MR Imaging and Drug Delivery. *Adv. Drug Delivery Rev.* **2008**, *60*, 1252–1265.
2. Peer, D.; Karp, J. M.; Hong, S.; Farokhzad, O. C.; Margalit, R.; Langer, R. Nanocarriers as an Emerging Platform for Cancer Therapy. *Nat. Nanotechnol.* **2007**, *2*, 751–760.
3. Riegler, J.; Nann, T. Application of Luminescent Nanocrystals as Labels for Biological Molecules. *Anal. Bioanal. Chem.* **2004**, *379*, 913–919.
4. Michalet, X.; Pinaud, F. F.; Bentolila, L. A.; Tsay, J. M.; Doose, S.; Li, J. J.; Sundaresan, G.; Wu, A. M.; Gambhir, S. S.; Weiss, S. Quantum Dots for Live Cells, *In Vivo* Imaging, and Diagnostics. *Science* **2005**, *307*, 538–544.
5. Resch-Genger, U.; Grabolle, M.; Cavaliere-Jaricot, S.; Nitschke, R.; Nann, T. Quantum Dots *versus* Organic Dyes as Fluorescent Labels. *Nat. Methods* **2008**, *5*, 763–775.
6. Astruc, D.; Lu, F.; Aranzaes, J. R. Nanoparticles as Recyclable Catalysts: The Frontier between Homogeneous and Heterogeneous Catalysis. *Angew. Chem., Int. Ed.* **2005**, *44*, 7852–7872.
7. Nann, T.; Skinner, W. M. Quantum Dots for Electro-optic Devices. *ACS Nano* **2011**, *5*, 5291–5295.
8. Shipway, A. N.; Katz, E.; Willner, I. Nanoparticle Arrays on Surfaces for Electronic, Optical, and Sensor Applications. *ChemPhysChem* **2000**, *1*, 18–52.
9. Indrasekara, A. S. D. S.; Paladini, B. J.; Naczynski, D. J.; Starovoytov, V.; Moghe, P. V.; Fabris, L. Dimeric Gold Nanoparticle Assemblies as Tags for SERS-Based Cancer Detection. *Adv. Healthcare Mater.* **2013**, *2*, 1370–1376.
10. Yim, T.-J.; Wang, Y.; Zhang, X. Synthesis of a Gold Nanoparticle Dimer Plasmonic Resonator through Two-Phase-Mediated Functionalization. *Nanotechnology* **2008**, *19*, 435605.
11. Cheng, Y.; Wang, M.; Borghs, G.; Chen, H. Gold Nanoparticle Dimers for Plasmon Sensing. *Langmuir* **2011**, *27*, 7884–7891.
12. Liu, X.; Lee, C.; Law, W.-C.; Zhu, D.; Liu, M.; Jeon, M.; Kim, J.; Prasad, P. N.; Kim, C.; Swihart, M. T. Au–$Cu_{2-x}Se$ Heterodimer Nanoparticles with Broad Localized Surface Plasmon Resonance as Contrast Agents for Deep Tissue Imaging. *Nano Lett.* **2013**, *13*, 4333–4339.
13. Zhao, N.; Li, L.; Huang, T.; Qi, L. Controlled Synthesis of PbS–Au Nanostar–Nanoparticle Heterodimers and Cap-like Au Nanoparticles. *Nanoscale* **2010**, *2*, 2418–2423.
14. Nakhjavan, B.; Tahir, M. N.; Natalio, F.; Gao, H.; Schneider, K.; Schladt, T.; Ament, I.; Branscheid, R.; Weber, S.; Kolb, U.; *et al.* Phase Separated Cu@Fe_3O_4 Heterodimer Nanoparticles from Organometallic Reactants. *J. Mater. Chem.* **2011**, *21*, 8605–8611.
15. Jiang, J.; Gu, H.; Shao, H.; Devlin, E.; Papaefthymiou, G. C.; Ying, J. Y. Bifunctional Fe_3O_4–Ag Heterodimer Nanoparticles for Two-Photon Fluorescence Imaging and Magnetic Manipulation. *Adv. Mater.* **2008**, *20*, 4403–4407.
16. Gschneidtner, T. A.; Fernandez, Y. A. D.; Syrenova, S.; Westerlund, F.; Langhammer, C.; Moth-Poulsen, K. A Versatile Self-Assembly Strategy for the Synthesis of Shape-Selected Colloidal Noble Metal Nanoparticle Heterodimers. *Langmuir* **2014**, *30*, 3041–3050.
17. Fernandez, Y. D.; Sun, L.; Gschneidtner, T.; Moth-Poulsen, K. Research Update: Progress in Synthesis of Nanoparticle Dimers by Self-Assembly. *APL Mater.* **2014**, *2*, 010702.
18. Wang, B.; Li, B.; Zhao, B.; Li, C. Y. Amphiphilic Janus Gold Nanoparticles *via* Combining "Solid-State Grafting-To" and "Grafting-From" Methods. *J. Am. Chem. Soc.* **2008**, *130*, 11594–11595.
19. Hermans, T. M.; Broeren, M. A. C.; Gomopoulos, N.; van der Schoot, P.; van Genderen, M. H. P.; Sommerdijk, N. A. J. M.; Fytas, G.; Meijer, E. W. Self-Assembly of Soft Nanoparticles with Tunable Patchiness. *Nat. Nanotechnol.* **2009**, *4*, 721–726.
20. Dong, B.; Li, B.; Li, C. Y. Janus Nanoparticle Dimers and Chains *via* Polymer Single Crystals. *J. Mater. Chem.* **2011**, *21*, 13155–13158.
21. Hofmann, A.; Schmiel, P.; Stein, B.; Graf, C. Controlled Formation of Gold Nanoparticle Dimers Using Multivalent Thiol Ligands. *Langmuir* **2011**, *27*, 15165–15175.
22. Homberger, M.; Schmid, S.; Timper, J.; Simon, U. Solid Phase Supported "Click"-Chemistry Approach for the Preparation of Water Soluble Gold Nanoparticle Dimers. *J. Cluster Sci.* **2012**, *23*, 1049–1059.
23. Groschel, A. H.; Walther, A.; Lobling, T. I.; Schacher, F. H.; Schmalz, H.; Muller, A. H. E. Guided Hierarchical Co-assembly of Soft Patchy Nanoparticles. *Nature* **2013**, *503*, 247–251.
24. Salvador-Morales, C.; Valencia, P. M.; Gao, W.; Karnik, R.; Farokhzad, O. C. Spontaneous Formation of Heterogeneous Patches on Polymer–Lipid Core–Shell Particle Surfaces during Self-Assembly. *Small* **2013**, *9*, 511–517.
25. Huang, T.; Nallathamby, P. D.; Xu, X.-H. N. Photostable Single-Molecule Nanoparticle Optical Biosensors for Real-Time Sensing of Single Cytokine Molecules and Their Binding Reactions. *J. Am. Chem. Soc.* **2008**, *130*, 17095–17105.
26. Gschneidtner, T. A.; Diaz Fernandez, Y. A.; Moth-Poulsen, K. Progress in Self-Assembled Single-Molecule Electronic Devices. *J. Mater. Chem. C* **2013**, *1*, 7127–7133.
27. Dewi, M.; Skinner, W.; Nann, T. Synthesis and Phase Transfer of Monodisperse Iron Oxide (Fe_3O_4) Nanocubes. *Aust. J. Chem.* **2013**, *67*, 663–669.
28. Zheng, Y.; Ma, Y.; Zeng, J.; Zhong, X.; Jin, M.; Li, Z.-Y.; Xia, Y. Seed-Mediated Synthesis of Single-Crystal Gold Nanospheres with Controlled Diameters in the Range 5–30 nm and Their Self-Assembly upon Dilution. *Chem.—Asian J.* **2013**, *8*, 792–799.
29. Dewi, M. R.; Laufersky, G.; Nann, T. A Highly Efficient Ligand Exchange Reaction on Gold Nanoparticles: Preserving Their Size, Shape and Colloidal Stability. *RSC Adv.* **2014**, *4*, 34217–34220.
30. Hermanson, G. T. *Bioconjugate Techniques*; Academic Press: New York, 1996.
31. Lu, A.-H.; Salabas, E. L.; Schüth, F. Magnetic Nanoparticles: Synthesis, Protection, Functionalization, and Application. *Angew. Chem., Int. Ed.* **2007**, *46*, 1222–1244.